Invited for **Mechanical Properties of Nanocrystalline Materials**
Edited by J.C.M. Li ; Pan Stanford Publishing, C/o World Scientific Publishing Co., Inc., Hackensack, NJ, 2009

CHAPTER 3

STRENGTH AND STRAIN RATE SENSITIVITY OF NANOPOLYCRYSTALS

Ronald W. Armstrong

Center for Energetic Concepts Development
Department of Mechanical Engineering
University of Maryland
College Park, MD 20742, U.S.A.
E-mail: rona@umd.edu

The strength and strain rate sensitivity properties of nanopolycrystals are attributed, at effective low temperatures, to a combination of Taylor-type, dislocation-density-based, deformation within the grain volumes and Hall-Petch-characterized obstacle resistance of the grain boundaries, consistent with results on conventional grain size materials but now scaled downwards even to single dislocation loop behavior. Because of the generally substantial grain boundary resistances associated with the yield point behaviors of bcc metals, only their grain volume deformation is thermally-activated. For fcc metals, there is thermal activation both of controlling dislocation intersections within the grain volumes and, especially, of needed cross-slip at higher local stresses in the grain boundary regions, thus providing an increasingly larger strain rate sensitivity at smaller grain sizes. Certain hcp metals follow a bcc-like behavior but, for others, the thermally-activated grain boundary resistances and enhanced nanopolycrystal strain rate sensitivities are fcc-like and controlled by the local operation of prism or pyramidal slip systems. Under effective high temperature, creep-like, conditions, an inverse Hall-Petch grain size dependence occurs and, then, the strain rate sensitivity is predicted to be smaller at smaller grain size.

1. Introduction

The current importance attached to investigating the deformation properties of nanopolycrystal materials has substantiated the assertion that "There are exciting reasons for investigating the strength properties of ultrafine grain metals both from an experimental and theoretical point of view."[1] In Ref. 1, emphasis was given to extension of the experimental Hall-Petch (H-P) observation that higher strengths were to be obtained for ultrafine grain size metals at effective lower temperatures and opposite (creep-based) lower strengths were to be obtained at effective higher temperatures. Thus, it was proposed that advantage could be taken of the lower material strength during high temperature fabrication and then additional advantage would be gained with a stronger material in the design application. From a theoretical viewpoint, emphasis was given to finer grain size material properties producing: (1) easier distinctions between continuum and discrete dislocation model descriptions of strength properties; and, (2) greater differences between alternative dislocation mechanisms proposed for quantifying the properties.

Figure 1 provides an updated description[2] on a log/log basis of the

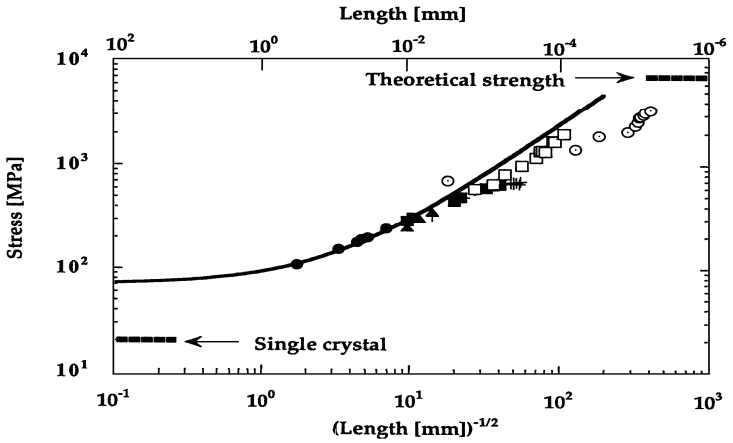

Fig. 1. The yield stress of iron and steel materials as a function of the inverse square root of their effective grain size, after T.R. Smith, *et al.*[2]

strength properties achieved over a range from conventional to ultrafine grain sizes for iron and steel materials. These material results are of special importance to begin with because Hall[3] and Petch[4] initially established an inverse square root of grain size dependence for the lower yield stress.

In the present chapter, the Hall-Petch (H-P) based dislocation pile-up model description proposed to explain the Fig. 1 results, and other similar results obtained for hcp and fcc metals, is combined with a thermal activation – strain rate analysis (TASRA) model description for interpreting the temperature and strain rate dependencies of nanopolycrystal material deformations. Experimental results are described, in addition to those for iron and steel shown in Fig. 1, for copper, magnesium, molybdenum, niobium, zinc, cadmium, aluminum, and nickel materials.

2. The Hall-Petch Relation

The H-P relation was initially measured over a conventional range of grain sizes, say, between a largest grain diameter of ~1.0 mm and smallest diameter of ~10 microns, expressed in direct linear plots of lower yield stress *vs*. inverse square root of average grain diameter as

$$\sigma_y = \sigma_{0y} + k_y \ell^{-1/2} \tag{1}$$

In Eq. (1), σ_y is the lower yield stress, ℓ is the average grain diameter, and σ_{0y} and k_y are experimental constants[3, 4]. The log σ/log [length]$^{-1/2}$ representation of Fig. 1 is taken to be an appropriate method of plotting strength/grain size results, say, when a range in grain diameter of more than 100 times is covered. In this case, as can be seen in the figure, σ_y is essentially determined at larger grain diameters by the value of the constant friction stress, σ_{0y}, and, at very small grain diameters, a straight line H-P dependence of slope 1.0 is obtained.

In Fig. 1, the relatively low "Single crystal" reference stress of ~20 MPa was taken as 2 times the critical resolved shear stress reported for essentially pure iron crystals by Atshuler and Christian[5]. The upper limiting "Theoretical strength" was taken somewhat arbitrarily as E/30 in

which E is the Young's modulus for steel. The compiled experimental measurements cover conventional and nanopolycrystal results[1, 6-10]. The drawn H-P curve was taken from Ref. 6. Attention is directed particularly to both the open-square measurements made by Embury and Fisher[7], for which the effective length on the abscissa scale was determined from the interlamellar spacings of eutectoid steel materials; and, to the open-circle results of Jang and Koch[10], for which the length was determined from the average grain diameters of ball-milled iron material. Both nanopolycrystal materials show at the finest grain sizes a somewhat reduced H-P k_y value. The same result will be shown here to apply for other materials also, as will be connected even with an inverse H-P dependence observed in certain cases at grain diameters of length in the vicinity of ~10 nm and smaller.

3. The Thermal Activation – Strain Rate Analysis

The viscoplasticity behavior of polycrystal materials has a long-standing history leading to the "invention" of crystal dislocations and subsequent modeling of their generation and motion, as recently reviewed[11]. For our purpose, important references are to articles by Orowan[12], Schoeck[13], Li[14], and Armstrong[15]. At conventional internal dislocation shear strain rates, say, of $\sim 10^{-4}$ to $\sim 10^{+4}$ s^{-1}, less than those involved in shock loading, there is control of the externally measured strain rate by the average dislocation velocity, v, in the expression[12]

$$d\gamma/dt = \rho b v \qquad (2)$$

In eq. (2), $d\gamma/dt$ is the resolved shear strain rate determined by an average mobile dislocation density, ρ, with Burgers vector, b, moving at an average velocity, v. The dislocation velocity, in turn, is taken to be thermally-activated through overcoming a Gibbs free energy barrier, G_0, with assistance of a thermal component of stress, τ^*, in the expression[13]

$$d\gamma/dt = (\rho b v_0)\mathbf{exp}\{-(G_0 - \int bA^* d\tau^*)/k_B T\} \qquad (3)$$

In Eq. (3), v_0 is the reference upper limiting dislocation velocity, A^* is the dislocation activation area, k_B is Boltzmann's constant and T is absolute temperature. The activation area is a critical parameter relating

to the strain rate sensitivity (SRS) of thermally-activated plasticity, as characterized also by the activation volume, $V^* = bA^*$, in the relation

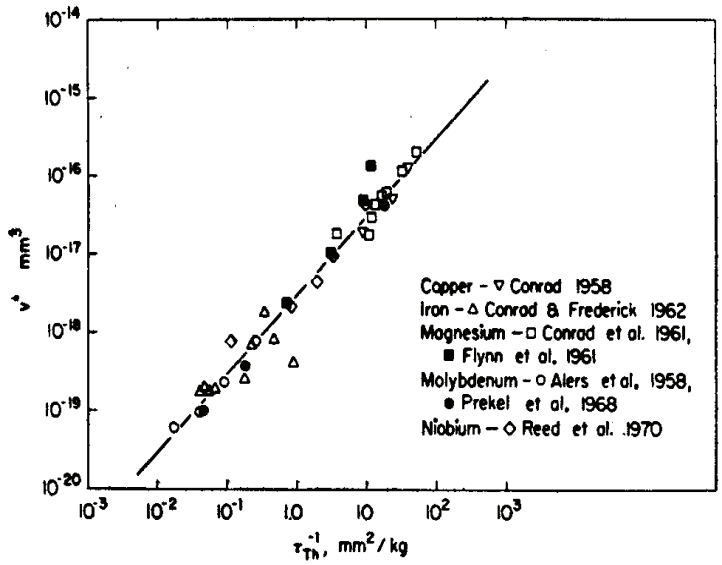

Fig. 2. Thermal activation volume, V^*, measurements compiled for a number of metals as a function of τ_{Th}^{-1} ($= \tau^{*-1}$ in the text), as reported by Armstrong[15]; 1 kg/mm^2 = 9.81 MPa.

$$V^* = k_B T[\partial \mathbf{ln}(d\gamma/dt)/\partial \tau^*]_T \qquad (4)$$

Li[14] has described thermodynamic aspects of the dislocation velocity dependence on shear stress and hydrostatic pressure for dynamic plasticity and high temperature creep conditions, respectively. Of interest here, as will be described, is the connection with an alternative power law relationship involving the velocity stress exponent, m^*, in

$$v = B(\tau^*)^{m^*} \qquad (5)$$

with B being constant; which relation is a suitable condensation of v in Eq. (3) when the shear based activation area, A^*, follows an inverse proportionality to τ^*. Figure 2 shows a compilation of such inversely proportional measurements[16-22] in terms of $V^* = bA^*$ as reported in the TASRA description given by Armstrong[15]. In agreement with Eq. (5), Prekel and Conrad[21] determined a linear log/log dependence of v on τ^*

over more than three orders of magnitude of v. Zerilli and Armstrong[23] employed the inverse dependence of V^* on τ^* in development of the so-called Z-A constitutive equations employed for material dynamics calculations[24]. It's important to note[22] that it's τ^*, the thermal shear stress component, and not τ, the total shear stress, in Eq. (5). Also, as will be made use of in the present report, the open square measurements for magnesium in Fig. 2 apply for basal (0001)[11-20] slip[18] whereas the closed square measurements are for prism (10-10)[11-20] slip[19].

4. The Hall-Petch Based Dislocation Pile-up Model

Further application of the dislocation pile-up analysis to explaining an H-P dependence of the yield stress of bcc, fcc and hcp metals with or without a yield point and of the flow stress at constant values of strain, σ_ε, led to the model relationship[6]

$$\sigma_\varepsilon = m\tau_{0\varepsilon} + mk_{s\varepsilon}\ell^{-1/2} \tag{6}$$

In Eq. (6), m is an orientation factor of the type originally described by Taylor for grain volume deformations within a polycrystal[25], $\tau_{0\varepsilon}$ is the critical resolved shear stress for multi-slip within the grains, for example, as described by Kocks[26], and $k_{s\varepsilon}$ is the microstructural shear stress intensity characterizing the average grain boundary resistance to plasticity spreading between the grains[8]. In relation to Eq. (1), now $m\tau_{0\varepsilon} = \sigma_{0\varepsilon}$ and $mk_{s\varepsilon} = k_\varepsilon$. The determination of $\sigma_{0\varepsilon}$ and k_ε values over the full stress – strain behavior of mild steel materials was described by Armstrong[27].

The potential temperature and strain rate dependencies of σ_ε that are implicitly contained in the modeled H-P relation are in $\sigma_{0\varepsilon}$ and k_ε. For $\sigma_{0\varepsilon}$,

$$\sigma_{0\varepsilon} = m[\tau_{o\varepsilon G} + \tau_{0\varepsilon}^*] \tag{7}$$

in which $\tau_{0\varepsilon G}$ and $\tau_{0\varepsilon}^*$ are the athermal and thermal components of the grain volume resolved shear stress, respectively, in the manner described by Seeger[28]. The result obtained for k_ε from the dislocation pile-up model is[8]

$$k_\varepsilon = m[\pi m_s G b \tau_c / 2\alpha]^{1/2} \quad (8)$$

in which m_s is a Sachs orientation factor, G is the shear modulus, τ_c is the local resolved shear stress needed in the grain boundary region, and α is the average orientation factor between edge and screw characterizations of the dislocation stress. In Eq. (8), τ_c has its own athermal and thermal stress components also in the same manner as given for Eq. (7). Equations (7) and (8) build onto the original Taylor idea[25] of relating

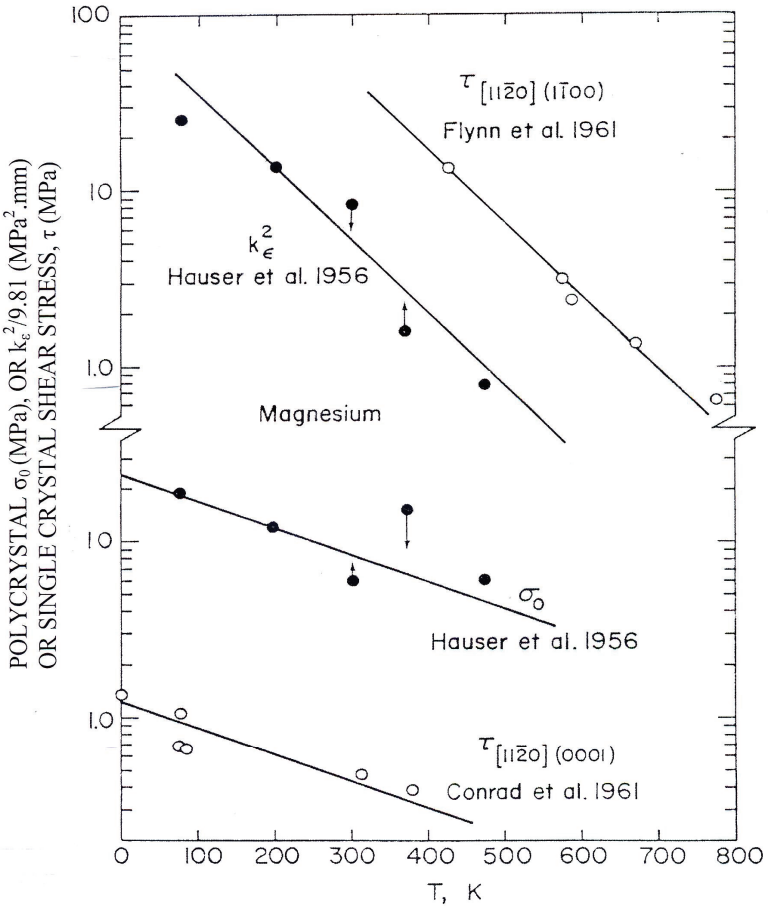

Fig. 3. Match for polycrystal and single crystal magnesium materials of the temperature dependencies for H-P parameters σ_0 and k_ε^2 with basal slip system and pyramidal slip system shear stresses, respectively, as adapted from Armstrong[30].

single crystal and polycrystal flow stresses not in terms of a single factor *m* making the connection but through consideration of the coupled stress requirements within the grain volumes and at the grain boundaries[29].

4.1. Application to hcp polycrystal deformations

Figure 3 shows for magnesium the match both of the temperature dependence of σ_o for an initial proof stress at yield and that of τ_0 for the basal slip system[18] as well as of k_ε^2 with that of τ_c for the prism slip system[19, 30]. The H-P constants were determined from the measurements reported by Hauser, Landon and Dorn[31] who had concluded from metallographic observations that prism slip appeared to be a main factor in controlling the local accommodation of strains in the grain boundary regions[32]. Thus in Fig. 3, a basal slip stress of ~0.3 MPa, or greater, operates on average on dislocation pile-ups within the grain volumes to produce a local shear stress of ~40 MPa in the grain boundary regions so as to activate the prism slip system.

Prasad, Madhava and Armstrong[33] showed for compressive stress measurements made on polycrystal zinc that the temperature dependence of $\sigma_{0\varepsilon}$ followed that of τ_0 for the basal (0001)[11-20] slip system and k_ε^2 followed the τ_0 (= τ_C) for the pyramidal (11-23}[11-22] slip system, utilizing for the two cases the single crystal shear stress measurements reported by Wielke[34] and by Soifer and Shteinberg[35], respectively. In this case, somewhat lower $\sigma_{0\varepsilon}$ measurements were obtained at temperatures of 100 K and lower because of the incidence of pile-up induced cleavage cracking that was confined within isolated grains. For zinc, the basal and pyramidal shear stresses are quite comparable at 300 K but that for pyramidal slip increases much more strongly as the temperature decreases. Thus, a strong increase in k_ε develops until full cleavage cracking intervenes; and, a well-established H-P relation is then observed for the tensile cleavage fracture stress[36]. Mannan and Rodriguez[37] established a similar k_ε^2 dependence matching τ_0 for pyramidal slip as a function of temperature for the H-P behavior of cadmium material.

4.2. Application to fcc polycrystal deformations

To begin with, it should be mentioned that the deformation properties of aluminum were studied extensively in the early twentieth century both in single crystal, multi-crystal, and polycrystal forms, as were reviewed not so long ago[29]. And, a compilation of the ambient temperature H-P measurements[38, 39] for aluminum provide the lowest H-P microstructural stress intensity, k_ε, values among the metal systems, for example, a value of ~1 MPa.mm$^{1/2}$ applies for aluminum as compared with ~5 for an interesting comparison to be made of copper and nickel behaviors, ~10 for magnesium, and ~24 MPa.mm$^{1/2}$ for iron. The reason for the low k_ε value for aluminum[38] is that cross-slip is the locally controlling stress for plastic flow transmission between the polycrystal grains of fcc metals and cross-slip occurs easily in aluminum at room temperature.

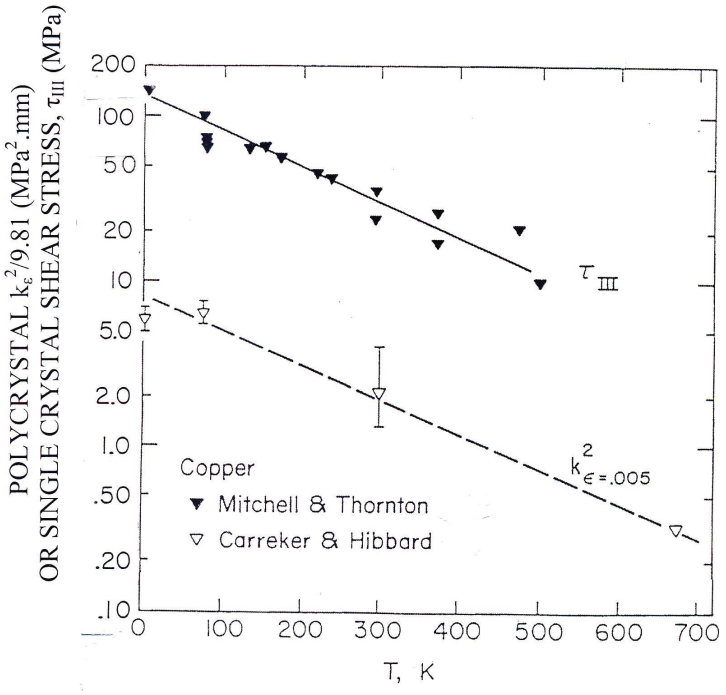

Fig. 4. A comparison of the temperature dependencies for the cross-slip stress, τ_{III}, and H-P k_ε^2 of copper, as obtained from measurements reported by Mitchell and Thornton[43] and by Carreker and Hibbard[41] respectively.

For aluminum, with $m = 3.1$, $m_s = 2.2$, $G = 25$ GPa, $\tau_c = \tau_{III} = 4.7$ MPa from Bell[40], $b = 0.29$ nm, and $\alpha = 0.8$, a low value of $k_\varepsilon = 1.2$ MPa.mm$^{1/2}$ is calculated from Eq. (8). Further evidence for fcc cross-slip control is provided by the comparison of approximately equal k_ε values being obtained from H-P plots of measurements reported for copper[41] and nickel[42], including in the latter case, an early result for nanopolycrystal material. Consider in Eq. (8) that the shear modulus of nickel is approximately two times greater than the shear modulus of copper, 76 GPa as compared with 40 GPa, but the ambient temperature cross-slip stress, τ_{III}, for nickel is approximately one-half that of copper[40], ~17 MPa as compared with ~30 MPa, so that the H-P k_ε values are approximately equal; see also later Ref. 65.

Figure 4 shows a comparison of the temperature dependencies of τ_{III} and k_ε^2 for copper as obtained from results reported by Mitchell and Thornton[43] and by Carreker and Hibbard[41], respectively. The open

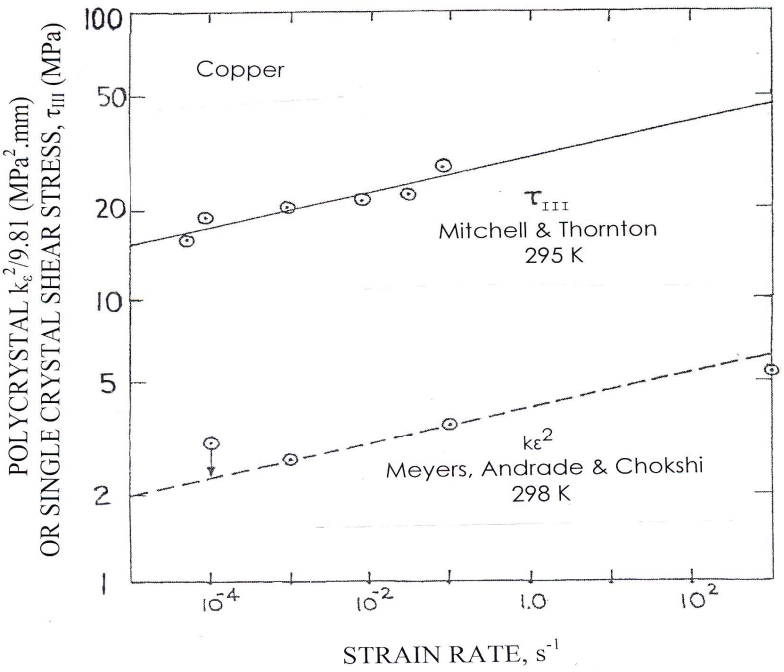

Fig. 5. A comparison of the strain rate dependencies for the cross-slip, τ_{III}, and H-P k_ε^2 of copper, as obtained from Mitchell and Thornton[43] and Meyers, Andrade and Choksi[45] measurements.

triangle point for k_ε^2 at 300 K is the average of estimations made both from the Carreker and Hibbard results and from an H-P plot[6] of other measurements reported by Feltham and Meakin[44].

Figure 5 shows a corresponding comparison on a strain rate basis at ambient temperatures of the Mitchell and Thornton[43] cross-slip, τ_{III}, measurements and k_ε^2 measurements reported by Meyers, Andrade and Chokshi[45]. In this case, the Meyers, Andrade and Chokshi measurement of k_ε^2 at $\sim 10^{-4}$ s^{-1} is indicated in Fig. 5 to be displaced downward so as to be in agreement with the corresponding range values indicated in Fig. 4.

5. The Strain Rate Sensitivity Dependence on Grain Size

The preceding results obtained for a thermally-activated dependence both in $\sigma_{0\varepsilon}$ and k_ε for hcp magnesium, zinc and cadmium and for fcc copper naturally lead to expectation of an H-P type grain size influence on the strain rate sensitivity. But why hadn't such an effect been observed in the many H-P research investigations made earlier on iron and steel materials, in which case only σ_{0y} is known to be thermally-activated? The main reason appears to be that the high value of $k_y \sim 24$ MPa.mm$^{1/2}$ associated with the yield point behavior is too high for easily discernable thermally-activated influence, as is true even for the higher athermal measurements of $k_T \sim 90$ MPa.mm$^{1/2}$ for deformation twinning[46] and $k_C \sim 100$ MPa.mm$^{1/2}$ for cleavage[47] of iron and steel materials. For example, with $k_y = 24$ MPa.mm$^{1/2}$, $m = 2.9$, $m_s = 2.2$, $G = 80$ GPa, $b = 0.27$ nm and $\alpha = 0.84$, a relatively high value of $\tau_c = 830$ MPa is obtained for Cottrell locking of dislocations at grain boundaries in iron. On the other hand, Fisher and Cottrell[48] have reported lower values of thermally dependent k_y measurements for the special case of quench-aged iron material. The situation for iron and steel was reviewed by Petch[49] in a comprehensive assessment of the theory of grain size influences on the yield point and strain ageing behaviors.

The combination of Eqs. (6) – (8) provides for evaluation of V^{*-1} for a polycrystal in terms of both $\sigma_{0\varepsilon}$ and k_ε contributions as[15, 50]

$$V^{*-1} = (mk_BT)^{-1}[\partial\sigma_{0\varepsilon}/\partial \mathbf{ln}(d\gamma/dt)]_T + (k_\varepsilon/2mk_BT\tau_C)[\partial\tau_C/\partial \mathbf{ln}(d\gamma/dt)]_T \ell^{-1/2} \qquad (9)$$

A negligible dependence of τ_C on strain rate (or temperature) for bcc metals removes the grain size dependence in the second term on the right-hand side of the equation. Otherwise, with substitution of the respective grain volume V_0* and grain boundary V_C* quantities,

$$V^{*-1} = V_0^{*-1} + (k_\varepsilon/2m\tau_C V_C^*)\, \ell^{-1/2} \qquad (10)$$

In Eq. (10), the product $\tau_C V_C$* should be constant, as indicated in Fig. 2, so long as the athermal stress component of τ_C is not too large; and hence, an H-P type dependence should be observed for the grain size dependence of V^{*-1}.

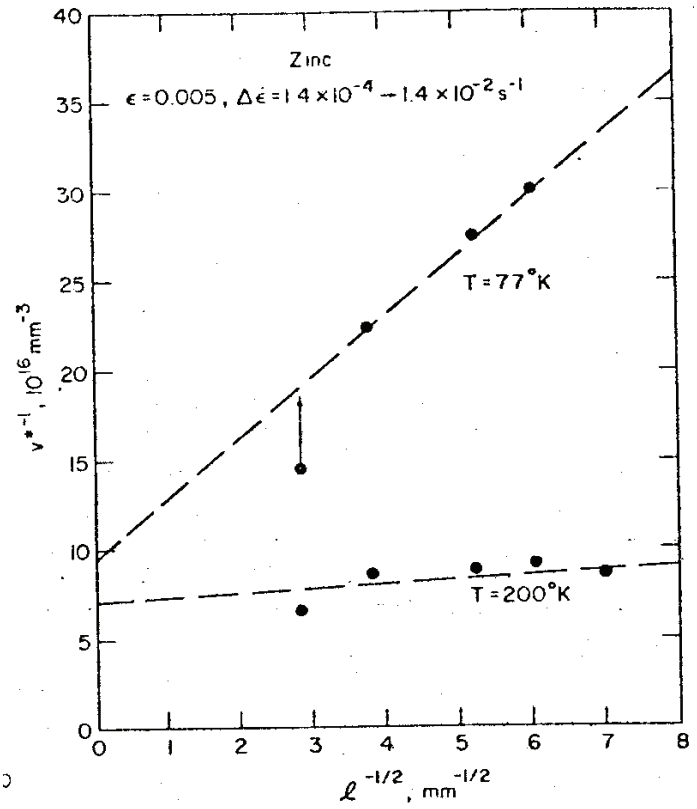

Fig. 6. H-P type V^{*-1} dependence of polycrystal zinc measured in compression at 200 and 77 K, as adapted from Prasad, Madhava and Armstrong[33].

5.1. Strain rate sensitivity for hexagonal close packed metals

Prasad and Armstrong[50] showed that pioneering measurements reported for cadmium by Risebrough and Teghtsoonian[51] followed Eq. (10). And, Fig. 6 demonstrates the application of Eq. (10) to strain rate change test performed in compression at two test temperatures for polycrystalline zinc material[33]. An extent of deformation twinning, favoring an increase in V^*, may have contributed to determining the

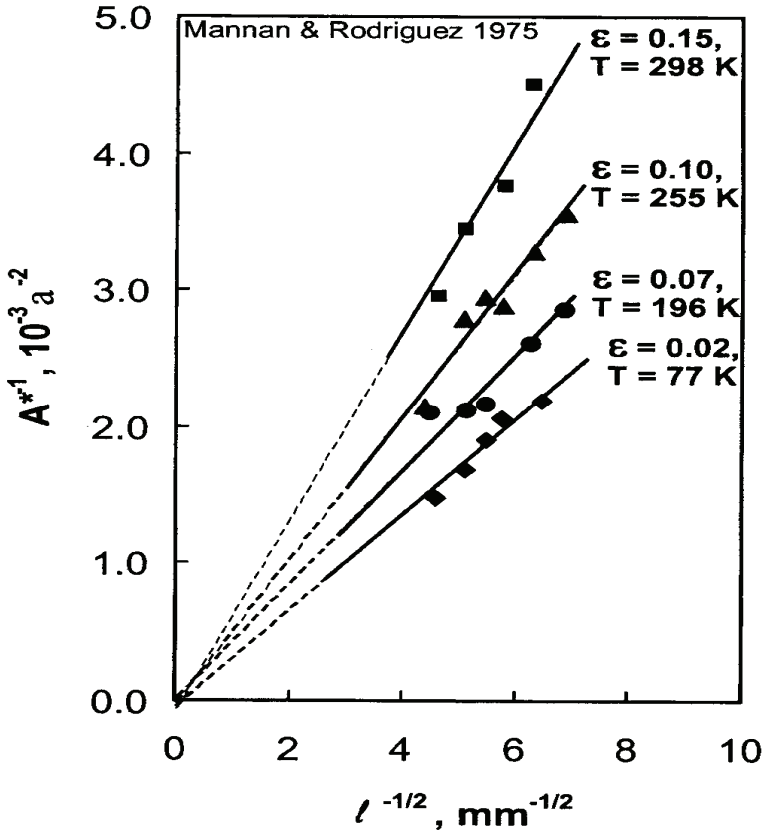

Fig. 7. Polycrystal cadmium measurements of A^{*-1} made by Rodriguez and Mannan[37] and showing an H-P type dependence on $\ell^{-1/2}$ at different strain values also tested at different temperatures, as adapted from results reported by Rodriguez, Armstrong and Mannan[52].

lower value of V^{*-1} at the larger grain size, as indicated by the upper-pointing arrow. The increased slope value of the V^{*-1} dependence was attributed to the increase in k_ε. By far, the larger increase in V^{*-1} is seen to be in the H-P grain size dependent term of Eq. (10).

In Fig. 7, A^{*-1} measurements made by Mannan and Rodriguez[37], as determined *via* $A^* = V^*/b$, on polycrystal cadmium material tested at different temperatures and at different strain values, are plotted on a same H-P type basis as for Fig. 6. The figure shows that the A_0^{*-1} value for cadmium is essentially zero. A quantitative analysis of the slope values both for the selected A^* measurements shown in Fig. 7 and for additional measurements obtained in the same investigation confirmed that the relevant activation area was that for pyramidal slip[52].

5.2. Strain rate sensitivity for face-centered cubic metals

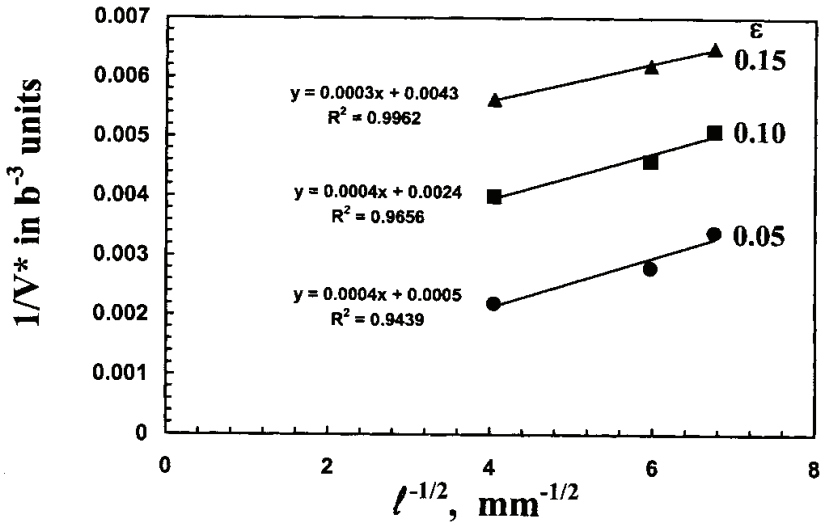

Fig. 8. Polycrystal measurements of V^{*-1} at 77 K for nickel reported by Narutani and Takamura[55] as expressed on an H-P type basis by Rodriguez[56].

Another reason for the strain rate sensitivity properties of fcc metals being of particular interest with regard to an influence of the polycrystal grain size, following on from the discussion in Section 4.2. of a low H-P k_ε being observed for aluminum, is that the fcc stress-strain properties

have a history of being correlated with a flow stress dependence on the square root of dislocation density, beginning from pioneering dislocation model calculations made by Taylor[25], for example, as related to his description of a (post-cross-slip) parabolic stress-strain curve for deformation results obtained on both single crystal and polycrystal aluminum materials. Ashby[53] has incorporated a dislocation density based grain size effect into the Taylor theory whereby an influence of grain size may be understood, especially relating to the accommodation of plastic strains via geometrically-necessary dislocations at grain boundaries. Kocks and Mecking[54] have provided an important review of the subject. Emphasis was given in the review to excellent results that were reported by Narutani and Takamura[55] on measuring a grain size dependence for the stress-strain properties of polycrystal nickel materials while also correlating the material stress-strain measurements with independently determined dislocation density measurements made *via* calibrated electrical resistivity measurements and with V^* measurements.

In Fig. 8, Rodriguez[56] has plotted on an H-P type V^{*-1} vs $\ell^{-1/2}$ basis the reported Narutani and Takamura measurements made at several values of strain; see Fig. 9 of Ref. 55. With a connection between V^* and the dislocation density made through $\rho \sim b^4/V^{*2}$, Narutani and Takamura obtained a lesser dependence of the flow stress on dislocation density than was obtained separately from the measurements made *via* electrical resistivity. Rodriguez pointed out that the problem was corrected by employing the (smaller) extrapolated values of V_0^{*-1} obtained on the ordinates axis in Fig. 8. Also, Rodriguez determined very much smaller values of V_C^* from the slope values of the V^{*-1} dependencies in Fig. 8 and showed the V_C^* values to be comparable with those associated with cross-slip, as had been reported by Puschl[57]. In a further connection with these important nickel results, Armstrong[29] established a quantitative H-P type relationship between separate strain-hardening results presented for 32 and 91 micron grain size materials. Thus, the Narutani and Takamura results in Fig. 8 are taken to be quantitatively compatible with an H-P dislocation pile-up model description. And, the two cases of fcc nickel in Fig. 8 and hcp cadmium in Fig. 7 present themselves as interesting opposite situations in which the strain rate sensitivity properties, at least at conventional grain sizes, are either mainly determined by the grain volume or the grain boundary properties, respectively.

5.3. Strain rate sensitivities at wider grain size range

The H-P type V^{*-1} dependencies shown in Figs. 6–8 extend to a conventional smallest grain size of ~20 microns and this is not an unusual smallest dimension for establishment of grain size dependent polycrystal strength properties. A more recent effort has dealt with the

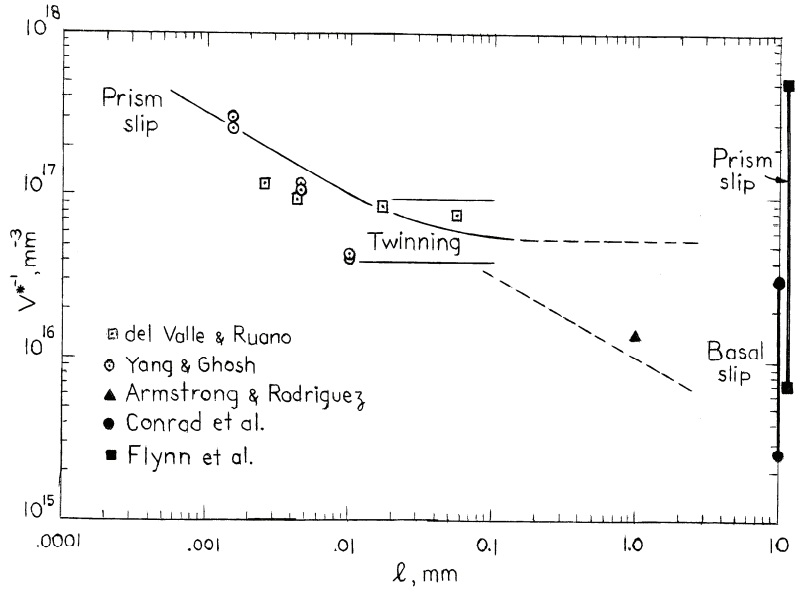

Fig. 9. V^{*-1} vs. ℓ for magnesium results[59] plotted on a log/log scale and referenced to single crystal measurements for basal[18] and prism[19] slip systems, as developed from the polycrystal results reported by del Valle and Ruano[60] and Yang and Ghosh[61].

wider attempt of connecting on a log/log scale, as for the strength evaluations in Fig. 1, conventional grain size V^{*-1} results with nanopolycrystal grain size results and, at the larger grain size limit, with single crystal measurements[2, 58]. Figure 9 shows one such connection begun for magnesium materials[59]. In the figure, the V^{*-1} dependence includes a combination of single crystal[18, 19] and polycrystal[60, 61] results extending downward in grain size near to the one-micron scale. The inclined solid and dashed line has a slope of -1/2 in accordance with prediction from Eq. (10). The open square points of del Valle and Ruano[60] correspond to tensile ε = 0.002 values determined for magnesium AZ31 alloy. In a further report, the authors determined a k_ε =

6.6 MPa.mm$^{1/2}$ value for the same strain[62]. A minor extent of twinning occurred at the largest grain sizes and became more prominent at larger strains. Yang and Ghosh[61] achieved smaller "ultrafine" grain sizes for the open circle points shown for the same alloy and found extensive twinning in compressive test results obtained on their larger 10 micron grain size material. A value of $k_\varepsilon \sim 4.0$ MPa.mm$^{1/2}$ has been estimated as an effective compressive stress value from their hardness measurements. Deformation twinning is known to be very nearly athermal in both hcp and bcc metals[46] because of the significant local twinning shear strain requirement determining τ_C in k_T, hence an amount of twinning involvement in the deformation behavior contributes to an increase in V^*. And, the experimental k_ε values for the materials in Fig. 9 are relatively low compared to a value of ~10 MPa.mm$^{1/2}$ that was originally determined for texture-free material by Hauser *et al.*[31], see Fig. 3 above, and confirmed in more recent measurements reported by Caceres and Blake[63] both for tensile and compression tests, thus confirming an absence of any significant influence of texture.

In Fig. 9, the filled triangle point plotted at $\ell = 1.0$ mm was calculated as a lowest possible value of $V^{*-1} = V_0^{*-1}$ for a single crystal from the linear relation $\tau_0^* V_0^* = 3.1 \times 10^{-20}$ J in Fig. 2 and taking $\tau_0^* = 0.4$ MPa from the measurements of Conrad *et al.*[18] that are shown in Fig. 3. Furthermore, with $\tau_C = 39$ MPa for prism slip in Fig. 3, $m = m_s = 6.5$ (from Ref. 6), $G = 17.5$ GPa, $b = 0.32$ nm, and $\alpha = 0.84$, a value of $k_\varepsilon = 10.6$ MPa.mm$^{1/2}$ is obtained from Eq. (8), in agreement with the results reported by Hauser *et al.*[31] and the recent determination by Caceres and Blake[63]. The reduction by half of the computed k_ε to an average $k_\varepsilon \sim 5.3$ MPa.mm$^{1/2}$ for the del Valle *et al.*[62] and Yang and Ghosh[61] results in Fig. 9, that are lower because of the material textures, produces an essentially equivalent grain size dependent contribution to V^{*-1} from the second V_C^{*-1} term in Eq. (10). By comparison of the Yang and Ghosh measurements made at their smallest grain size with the vertical ranges of V^{*-1} shown for the basal slip and prism slip systems at the right side ordinate axis of Fig. 9, it may be seen that the ultrafine polycrystal measurements, being free of deformation twinning, approach the highest prism slip values determined for the Flynn *et al.*[19] single crystal measurements.

A more pertinent example of investigating the relation of strain rate sensitivity and grain size at ultrafine grain sizes, this time extending to nanopolycrystal grain size measurements, is shown in Fig. 10 as developed by Armstrong and Rodriguez[65] in an H-P assessment of

important fcc results originally compiled for combined copper and nickel materials by Asaro and Suresh[64]. First, it should be noted again, as mentioned above in Section 4.2, that copper and nickel material strength results, that might be thought to be at somewhat different stress levels because of their very different elastic moduli, were in fact deemed to be quite comparable in terms of having approximately the same H-P k_ε values because of the model dislocation pile-up result of k_ε being proportional to the square root of the product of G and τ_{III}, which product has approximately the same value for the two materials. In the log/log

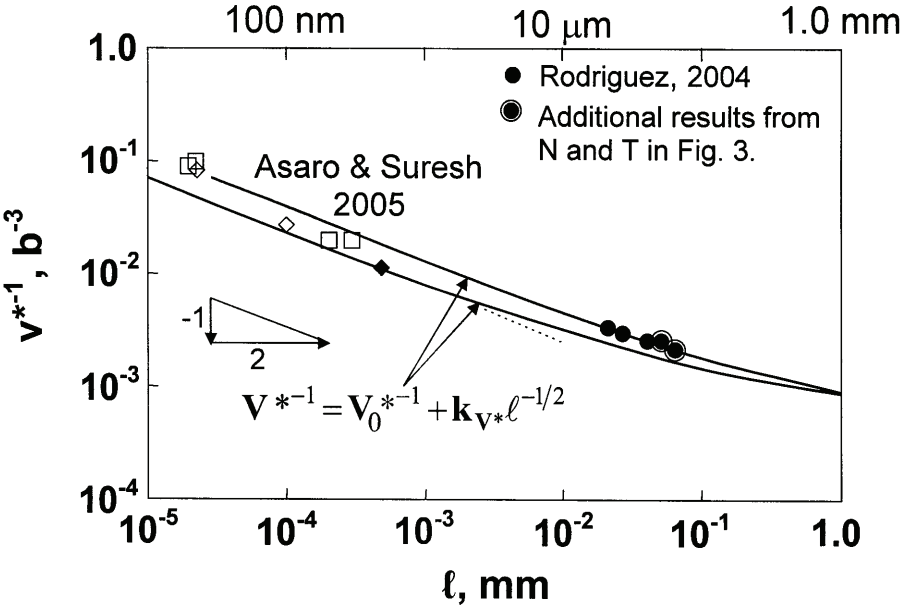

Fig. 10. A predicted H-P type V^{*-1} dependence shown on a log/log basis[65] to connect conventional ~10-to-100 micron scale V^{*-1} measurements made at 77 K, as reported for nickel[55], and compiled copper plus nickel results obtained at 295 K and including nanopolycrystal ~20-to-500 nm grain sizes[64]; "N and T" in the figure legend is for Narutani and Takamura[55] and "Rodriguez, 2004" is the present Ref. 56.

representation of Fig. 10, the V^{*-1} results determined by Rodriguez[56] from the Narutani and Takamura[55] measurements made for nickel at ε = 0.05 and 77 K are shown at their respective conventional grain sizes. And, the H-P relation from Eq. (10) drawn through the Narutani and

Takamura points is extended into the nanoscale regime both for the 77 K temperature of the measurements and, also, is drawn for 295 K as estimated through employment of a lowered value of k_ε to match the 295 K temperature of the compiled Asaro and Suresh measurements[64]. The H-P based connection of V^{*-1} results is thus established by a single H-P type relationship despite an order of magnitude difference that is shown between $V^* \sim$ 100-1000 b^3 at conventional grain sizes and $V^* \sim$ 10-100 b^3 at nanopolycrystal grain sizes.

It's also of interest that Asaro and Suresh employed a power law expression for the stress dependence on strain rate, in line with Eq. (5) above but instead employing the total stress, σ, in place of τ^*, and a numerical value, $\sqrt{3}$, in place of the Taylor factor, m. Thus, for this case, the strain rate sensitivity is specified in terms of the exponent, $m^{*\prime}$, as

$$m^{*\prime} = [\partial \mathbf{ln}(d\gamma/dt)/\partial \mathbf{ln}\tau]_T = \sqrt{3}[k_B T/\sigma V^*]_T \qquad (11)$$

On such different basis for $m^{*\prime}$, Armstrong and Rodriguez[65] showed that the parameter should be contained within the limits,

$$\sqrt{3}[k_B T/\sigma_0 V_0^*] < m^{*\prime} < \sqrt{3}[k_B T/2m\tau_{III}\, V_{III}^* \qquad (12)$$

Reasonable correlation was made between the limiting estimations of Ineqs. (12) and the range of the reported measurements. Other copper nanopolycrystal measurements[66, 67] have been reported very recently on the same power law basis as employed by Asaro and Suresh.

6. Hall-Petch Strengths for Nanopolycrystals

Meyers, Mishra and Benson[68] have done a comprehensive review of the mechanical properties of nanocrystalline materials, including a compilation of 374 references. Attention was given to experimental observations of V^* decreasing in the nanopolycrystal regime for fcc metals while, for bcc metals, V^* remains constant at the relatively low value observed for conventional grain size materials. Conflicting observations were reported for the influence of grain size in creep testing. A considerable number of experimental results were described for the influence of a reduction in grain size on improving material strength properties. The subject is added-to here on an H-P dislocation

pile-up model basis and includes consideration of both grain size strengthening in an effective low temperature condition and grain size weakening at effective higher temperatures[1, 69, 70].

6.1. The pile-up model extension for strength properties

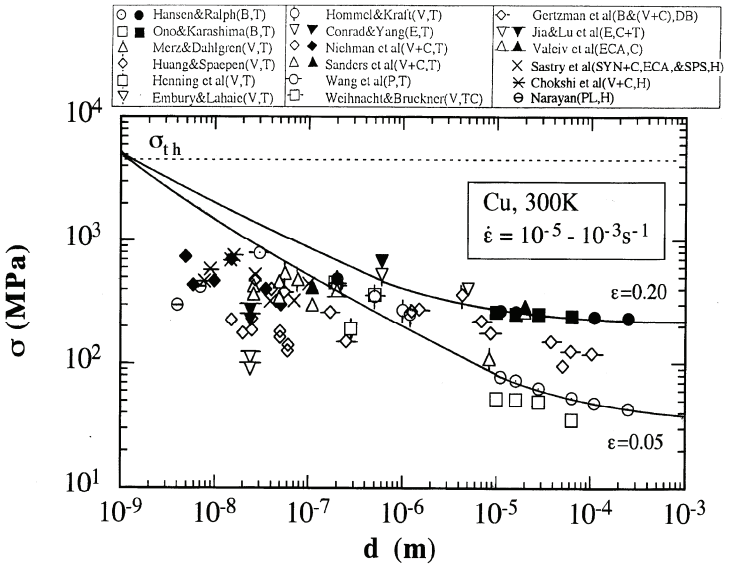

Fig. 11. A log/log presentation of the compilation by Conrad[71] of grain size dependent strength measurements for copper and including extended curves for the H-P dependence as described by Armstrong, Conrad and Nabarro[58]; d = ℓ in the present text.

In Fig. 11, a compilation of strength results reported by Conrad[71] are shown on a log/log basis with an extended superposition of H-P curves determined at the ε = 0.05 and 0.20 values as obtained from the careful investigation of Hansen and Ralph[72]. At 300 K and at the largest grain diameter ℓ (= d) ~ 1.0 mm, the ε = 0.05 plot of the flow stress is seen to continue to exhibit an influence of the $k_\varepsilon \ell^{-1/2}$ term whereas, both because of the reduced k_ε at ε = 0.20 and an increased strain hardening in the H-P $\sigma_{0\varepsilon}$ stress intercept, an essentially constant level of the flow stress is seen to be determined. And in the nanopolycrystal regime, the ε = 0.05 determined flow stress exhibits a predicted (-1/2) slope value that is not quite achieved for the ε = 0.20 flow stress curve because of the raised $\sigma_{0\varepsilon}$

value. Otherwise, the observation is easily made that the plotted nanopolycrystal stress measurements fall below the conventional H-P grain size extrapolation. And, for the individual studies where sufficient measurements at nanoscale grain sizes were obtained, the lower stresses involve reductions in both $\sigma_{0\varepsilon}$ and k_ε values. The interest here is to investigate the situation of the nanopolycrystal grain size having become sufficiently small that the strength is being determined ultimately by a single dislocation loop overcoming the grain boundary obstacle[73, 74].

Li and Liu[74] produced the pioneering computation for expansion of a circular dislocation loop against its own line tension and a grain boundary obstacle. The resultant stress is expressed as

$$\sigma = m[\tau_0 + (3Gb/4\pi\ell)\{(5/6)(\mathbf{ln}[4\ell/b] - 1) - 1/16\} + \tau_C] \qquad (13)$$

Eq. (13), though being only one of many pile-up type calculations described in an important review article by Li and Chou[75], is one made in

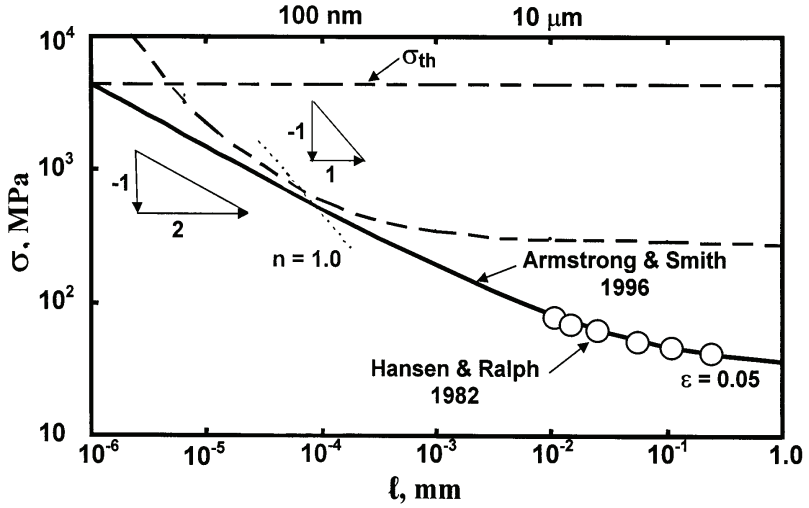

Fig. 12. Dislocation pile-up based Hall-Petch dependence for copper spanning a range in grain diameters from conventional to nanopolycrystal sizes and highlighting the transition to a single dislocation loop expanding against the grain boundary obstacle[65].

addition to another early calculation[76] anticipating future interest in nanopolycrystal strength properties. That issue and other model pile-up

applications to material strength properties have been reviewed by Armstrong[77], including a role for H-P influences on composite material properties. In Fig. 12, the dashed curve shown just above the H-P dependence established by Hansen and Ralph is that computed on the basis of their k_ε being employed in Eq. (10) to determine τ_C and then that τ_C employed in the evaluation of Eq. (13).

At the larger grain sizes shown in Fig. 12, the average number, n, of dislocations in the pile-ups accounts for the separation of the (solid) H-P

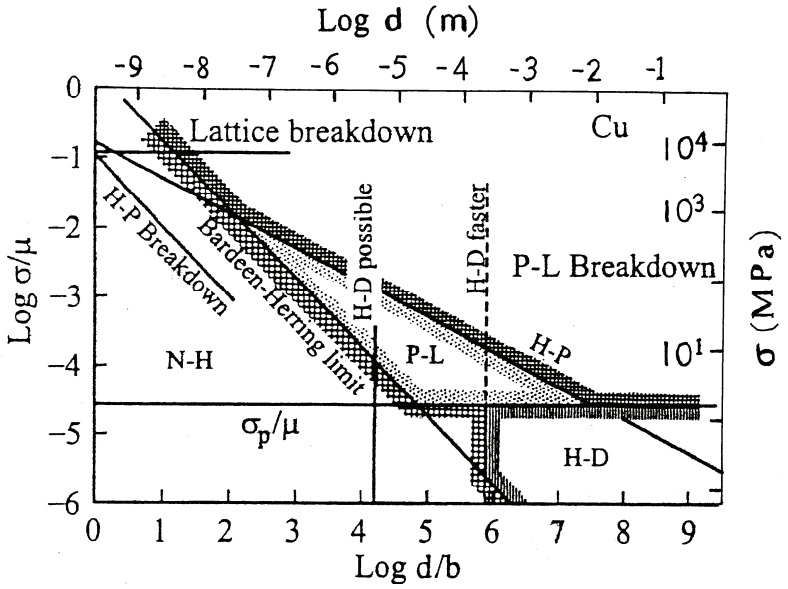

Fig. 13. The grain size dependence estimated for upper limiting creep stresses of copper, as adapted from Nabarro[78]; $\mu = G$, $d = \ell$, N-H is Nabarro-Herring, σ_p is the Peierls stress, *P-L* is for Power-Law type creep, and *H-D* is for Harper-Dorn type creep.

and (dashed) single dislocation curves. For example, at ℓ = 100 microns and with

$$n = 2\alpha k_\varepsilon \ell^{1/2}/\pi m G b \qquad (14)$$

as evaluated from Eq. (7) in Ref. 8 with substitution of $k_\varepsilon \ell^{-1/2}/m$ for the effective shear stress, $\tau_e = (\tau - \tau_{0\varepsilon})$, a number of dislocation loops $n \sim 26$ is spread on average across a typical grain. As the grain size is made smaller, n decreases until at n = 1.0 the H-P and dashed curves should

meet. This is marked by the dotted line of slope (-1) at ~100 nm where the solid and dashed curves reach a minimum separation rather than intersection because of the analytic approximation made in the continuum mechanics description on which Eq. (14) is based.

The results in Fig. 12 bear also on Figure 13 that has been adapted from a graphical description originally developed by Nabarro[78] to illustrate over a large range in grain size the upper limiting stress dependencies which might be achievable in creep tests[58], even including an upper limiting H-P dependence. Any friction type, $\sigma_{0\varepsilon}$, stresses are neglected in the figure. At stresses of the order of 1.0 MPa or less, below the Peierls-Nabarro stress, σ_p, Nabarro-Herring (N-H) creep should be observed at grain sizes of the order of ~100 microns or less; and, Harper-Dorn (H-D) creep would apply at larger grain sizes. A reciprocal grain diameter dependence for a Bardeen-Herring limit to creep is reached at higher stresses after which Power-Law (P-L) creep predominates. And in turn, the range in stress and grain size for P-L creep behavior is limited by an H-P dependence that breaks down to the reciprocal $(d/b)^{-1}$ Bardeen-Herring limit at a grain diameter below the same ~100 nm pile-up limit described for Fig. 12.

Presumably, logarithmic creep, as investigated in detail in the pioneering copper single crystal study reported by Conrad[16], and reviewed by Weertman[79] in relation to the other creep type constitutive equations, would apply at stresses above the limiting H-P dependence shown for P-L creep. In this regime, Armstrong[1, 69, 70] had reported on the grain size dependence of the plastic strain rate achieved at constant total stress but incorporating thermal activation in the H-P $\sigma_{0\varepsilon}$ friction stress. A main purpose was to make connection between effective low temperature grain size strengthening and effective high temperature (creep-type) grain size weakening behaviors[1]. The topic relates to modern interest in an inverse H-P dependence observed at the smallest nanopolycrystal grain sizes[68, 80].

6.2. Transition from grain size strengthening to weakening

Meyers *et al*.[68] have provided a list of model equations for the occurrence of grain size weakening under creep conditions. For example, the Nabarro-Herring behavior mentioned above in connection with Fig. 13 was given as

$$(d\varepsilon/dt)_{NH} = (A_{NH}D_L Gb/k_B T)(b/\ell)^2(\sigma/G) \qquad (15)$$

In Eq. (15), A_{NH} is a constant, D_L is the lattice diffusion coefficient, and the other symbols have already been defined. At constant strain rate, σ is proportional to ℓ^2 thus being reflective of grain size weakening behavior. Such model equation descriptions relate generally to the grain boundary regions being weaker either because of enhancement of mass transport by diffusion mechanisms as mentioned above or because of additional

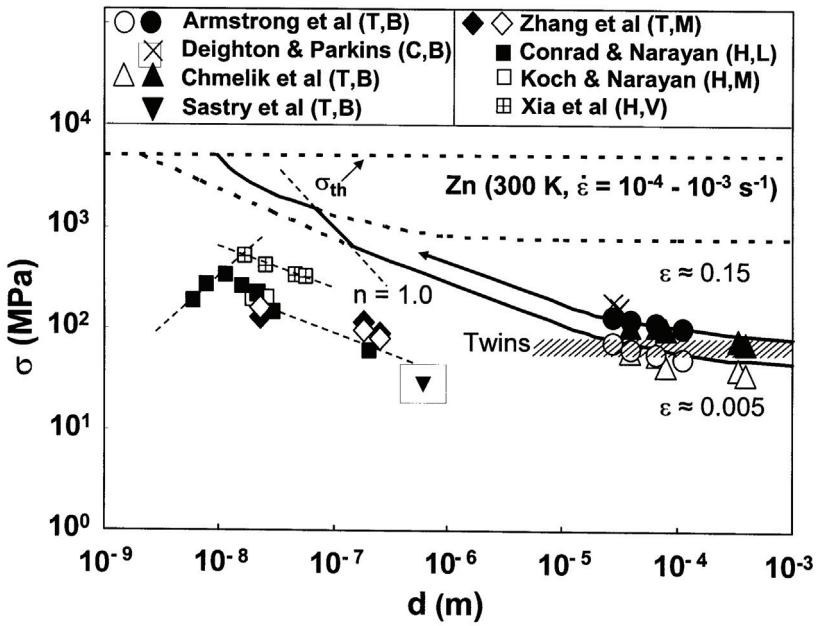

Fig. 14. Grain size strengthening and weakening measurements compiled for zinc materials by Conrad and Narayan[80] and connected with several H-P dependencies at nanopolycrystal and larger grain sizes *vs.* an inverse H-P dependence at the smallest grain sizes[81]; d = ℓ.

deformation mechanisms coming into play such as grain boundary shearing processes or even cracking or for all of these reasons[1, 68].

Figure 14 shows important H-P results compiled for zinc materials by Conrad and Narayan[80], including their own measurements made with

colleagues, and adapted[81] to include a number of dashed H-P lines[80, 82]. At the smallest nanopolycrystal grain sizes, an inverse H-P dependence is indicated. Beginning from the larger grain size end of the figure, parallel H-P dependencies from Ref. 6 at ε = 0.005 and 0.15 are shown to be extended into the nanopolycrystal regime with constant k_ε values. The transition to single loop expansion against the grain boundary resistance occurs again at a value of d (= ℓ) of ~100 nm. In the vicinity of this grain size and extending further downward to just larger than 10 nm, several sets of data[82-85] are shown also to follow H-P dependencies but, as mentioned above, at indicated lower k_ε values[81]. Below ~10 nm an inverse grain size weakening dependence is observed with an indicated power law dependence of slope 1.0. Conrad and Narayan[80] provided a detailed analysis of the total results, including those obtained with colleagues[83-85]. Particular consideration was given to an important influence at larger grain sizes of deformation twinning, as marked in the figure and especially relating to the twin-free observation of an increased V^{*-1} at smaller grain sizes in the H-P strengthening regime; see the discussion of twinning relating to the results in Fig. 9.

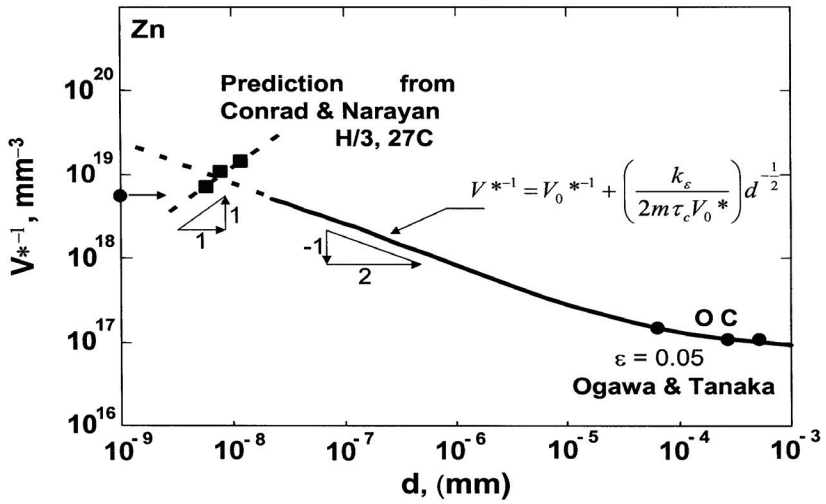

Fig. 15. A log/log graph of the H-P type V^{*-1} dependence on grain size extended into the nanopolycrystal regime for comparison both with prediction of an inverse H-P strain rate sensitivity dependence on grain size and an upper-limiting value shown on the ordinate scale of $V_C^{*-1} = b^{-3}$ for pyramidal slip[81]; H is hardness and d = ℓ.

Rodriguez and Armstrong[81] proposed a combination both of grain size strengthening and weakening explanations for the strain rate sensitivity results shown for zinc in Fig. 15. First, an H-P dependence was extended to the nanopolycrystal grain size regime from the excellent conventional polycrystal grain size measurements reported by Ogawa and Tanaka[86] for $\varepsilon = 0.05$ in compression tests made at 273 K. The solid curve for the H-P dependence is seen to end at the level of the (filled-circle) V^{*-1} value shown on the ordinate scale with arrow pointing to the H-P terminus. The point corresponds to calculation of an upper limiting value of $V^{*-1} = b^{-3} = 5.7 \times 10^{18}$ mm^{-3} for the (a +*c*) Burgers vector for pyramidal slip. At the smallest grain sizes, the several filled-square points have been plotted in accordance with a generalized grain size weakening constitutive equation prediction given by Langdon[87] as

$$(d\varepsilon/dt) = (AD_L Gb/k_B T)(b/d)^p(\sigma/G)^q \qquad (16)$$

In Eq. (16) that was ascribed to grain boundary shearing, *A*, *p* and *q* are experimental constants; see the similarity to Eq. (16) for Nabarro-Herring creep with $p = 2$ and $q = 1$. Even for the weakening case of grain boundary shearing, however, there may be roles to be played by dislocation pile-ups. Federov, Gutkin and Ovid'ko[88] have modeled the deformation of the grain boundary itself shearing against triple points *via* dislocation pile-ups that are contained within the boundary interfaces whereas Conrad[89] has proposed a constitutive equation for grain boundary strengthening in which case pile-ups from within the grains force grain boundary shearing to occur. The model considerations are indicative of progress that is being made in modeling the grain boundary deformation behavior, especially that for weakening behavior, in proceeding onwards from the situation described in Ref. 1 pertaining to "the difficulty of characterizing the structure of grain boundaries and the nature of the events which occur there".

Otherwise, for the zinc grain size weakening results of interest in Figs. 14 and 15, and with $p = q = 1.0$, V^{*-1} is evaluated from Eq. (16) as

$$V^{*-1} = \sigma/mk_B T \qquad (17)$$

With the several σ values determined from Fig. 14, the corresponding filled-square points in Fig. 15 were able to be computed. Thus, an interesting consequence of an inverse H-P dependence on grain size for

nanopolycrystals leads to prediction of a reversed grain size dependence of the strain rate sensitivity[81].

7. Discussion

The log/log H-P presentations in Figs. 11 and 14 are adapted from original versions presented by Conrad[71] and by Conrad and Narayan[80] as mentioned at the place of each figure introduction. Not shown in each case, are the divisions proposed to separate the grain size dependent results into separate mechanism dependent regions, for example, beginning from the largest grain sizes to include: I., a region primarily corresponding to main influence of the dislocation density; then, at smaller grain size, II., a region of H-P pile-up application; and, finally at smallest grain size, III. a region of inverse H-P behavior. In the present description, an H-P dependence has been argued to cover the full extent of regions I. and II., even including the transition to an H-P type dependence corresponding to expansion of a single dislocation loop against its own line tension and the grain boundary obstacle, as employed in the calculation made by Li and Liu[74]. At limiting larger grain sizes, however, for which $\sigma_{0\varepsilon} > k_\varepsilon \ell^{-1/2}$, it may be seen on the graphical log/log basis that the polycrystal flow stress is largely described by the Taylor-type influence of dislocation density that is contained in $\sigma_{0\varepsilon}$ and is associated only with a smaller apparent grain size dependence of σ_ε. Thus, there isn't a large difference between the stage I/II description given by Conrad and that proposed here.

A preference for the strain rate sensitivity being expressed in terms of V^{*-1}, see Eq. (4), or by the related m^* parameter, in Eq. (5), is made clear when the alternative $m^{*\prime}$ parameter, see the Ineqs. (11), is evaluated as

$$m^{*\prime} = mk_BT/\sigma_\varepsilon V^* \qquad (18)$$

Thus in Eq. (18), $m^{*\prime}$ is seen to depend inversely on the product of the total stress, σ_ε, and V^*, as mentioned above with regard to Eq. (5) and $m\tau^*$ for the thermally activated stress *vs.* $m\tau$ for the sum of grain volume and grain boundary terms on the right-hand side of Eq. (6). The σ_ε and V^* variables, for example, have separate dependencies on strain, for example, as reported[22] for single crystal niobium measurements. In that case, V^* was found to be independent of strain, as typical of a thermally-

activated Peierls stress dependence, and $m^{*\prime}$ followed the $\sigma_{\varepsilon}^{-1}$ dependence on ε. Beyond the limiting cases for $m^{*\prime}$ given in the Ineqs. (12), if $V_0^* > V_C^*$ as is generally true for the fcc case of dislocation intersections *vs*. cross-slip, and $\sigma_{0\varepsilon} < k_{\varepsilon}\ell^{-1/2}$ as is true at nanopolycrystal grain dimensions, then in the interim small grain size regime the grain size dependence may be approximated as

$$m^{*\prime} \sim (k_B T/2\tau_C V_C^*)\{1 - (\sigma_{0\varepsilon}/k_{\varepsilon}\ell^{-1/2})\} \qquad (19)$$

In Eq. (19), $m^{*\prime}$ increases as the grain diameter decreases. In several investigations, Della Torre *et al*.[90], Ghosh[91], and Wei[92], `have reported on details of experimentally measuring m*' and discussed its interpretation.

The reduction shown by the downward displacements of the several dashed H-P lines in Fig. 14, thus reflecting a decrease in k_{ε} for these zinc materials, is not untypical of the broader number of measurements made of nanopolycrystal behavior for other materials. Armstrong *et al*.[58] suggested that one reason for the observation could be that the grain boundary regions were more likely to be relatively disordered at nanometric grain size dimensions compared to conventional grain-sized materials. The suggestion was also put forward that the unusual observation of deformation twinning being observed in nanopolycrystal aluminum material might be the result of such twin nuclei being already present in the disordered grain boundary structures. Li[93] has modeled the potential influence of impurity and porosity effects on the equilibrium and non-equilibrium properties of nanopolycrystal grain boundaries. Narayan and Zhu[94] and Wu, Narayan and Zhu[95] have explained the observation of nanoscale twinning in terms of the partial dislocation structures present at boundaries in nickel and copper-5%germanium alloy, respectively, as made *via* model dislocation reaction descriptions matching their high resolution electron microscopy results. Evidence for nanopolycrystal grain boundaries being generally disordered seems to be an accepted observation at grain boundaries in molecular dynamics modeling of nanopolycrystal structures, for example, as described by Weertman *et al.*[96] and by Kadau *et al*.[97].

An interesting opposite consideration that may prove the case for nanoscale boundaries being generally disordered is provided by the role established in nanopolycrystals of relatively perfect twin boundaries contributing to a substantial H-P dependence. Asaro and Suresh[65] counted twin boundaries formed during material production in their

reported nanopolycrystal grain size measurements. The reported data lead to determinations of $k_y \sim 3.8$ MPa.mm$^{1/2}$ for the tensile test results and a compressive stress $k_\varepsilon \sim 4.3$ MPa.mm$^{1/2}$ determined for the reported hardness measurements. In follow-up results, Zhu, Samanta, Kim and Suresh[98] pointed out *via* atomistic reaction pathway computations applied to the obstacle nature of nano-twin boundaries in copper material that both significant H-P strengthening and high ductility, along with an increased strain rate sensitivity, were reasonable expectations for well-defined interfacial obstacles to transmission of plastic flow. The consideration of grain boundary characterizations relates also to boundary type discriminations made in an early investigation by Wyrzykowski and Grabski[39] for aluminum at ultrafine grain sizes.

Such positive H-P ductility connection mentioned above had been proposed earlier for conventional grain size material through the observation that the true fracture strain of magnesium and Armco iron materials followed an H-P type dependence[99, 100]. The result should be valid if the material work hardening is independent of grain size and mechanical instability doesn't intervene. In addition to the consideration of ductility dependence on grain size, there is the natural question of how an H-P dependence for the flow stress might also connect with other mechanical properties of nanopolycrystals, in the same manner as was considered earlier for fracture, hardness, creep, and fatigue properties[1, 27]. Zhu *et al.*[101] have co-edited a recent proceedings on ultrafine grained material mostly including both methods of producing the materials for engineering applications and evaluation of the resultant properties. Also, a review has been given by Song *et al.*[102] of higher strength and, especially higher fracture toughness properties being obtained for ultrafine grain size steels of ~1 micron grain size and smaller as achieved in traditional material compositions. Hwang *et al.*[103], and more recently, Bondar[104] have reported on the pronounced shear banding behavior associated with ultrafine grain size low carbon steels and copper materials, respectively, when subjected to dynamic loading. The results connect with other aspects of high rate loading behaviors described by Armstrong and Walley[11] for conventional and fine grained structural materials as well as by Armstrong[105] for a role of dislocation pile-ups in achieving advantageous deformation and energy release properties of small particle sizes in energetic (explosive) material composites.

8. Conclusion

The experimental H-P dependence observed for the yield and flow stresses of conventional grain size polycrystals, beginning with iron and steel materials, is shown to be useful for assessing nanopolycrystal strength and strain rate sensitivity behaviors for a larger selection of materials. The experimental H-P dependencies are interpreted in terms of the dislocation pile-up model that allows for transition at ultrafine grain size to a single dislocation loop expanding against the grain boundary resistance. In contrast to the yield-point-associated, higher, H-P k_ε values observed for bcc metals, those k_ε values for fcc and certain hcp metals are sufficiently low to be thermally-activated. In consequence, the reciprocal activation volume characterization of the strain rate sensitivity shows an H-P type dependence also that, therefore, is greatly enhanced at nanopolycrystal grain sizes. At the smallest grain sizes, there is evidence of the flow stress exhibiting an inverse H-P type dependence. And, the inverse dependence is attributed to the same type of grain boundary weakening character that is characteristic of effective high temperature creep. For this case, a reversed grain size dependence is predicted to occur also for the strain rate sensitivity.

Acknowledgments

Prof. J.C.M. Li is thanked for inviting the present article that has benefitted from key research results of his that were obtained with colleagues and students. Dr. Stephen Walley, University of Cambridge, is thanked for providing very useful reference articles. Otherwise, a number of the results described in the present report were achieved as part of a cooperative research project underway with Prof. Placid Rodriguez, Indian Institute of Technology, Madras, and whose sudden death on 31 August, 2008, is very sadly noted.

References

1. R.W. Armstrong, in *Ultrafine–Grain Metals; Sixteenth Sagamore Army Materials Research Conference*, Eds. J.J. Burke and V. Weiss (Syracuse University Press, N.Y., 1970) p. 1.

2. T.R. Smith, R.W. Armstrong, P.M. Hazzledine, R.A. Masumura and C.S. Pande, in *Grain Size and Mechanical Properties – Fundamentals and Applications*, Eds. M.A. Otooni, R.W. Armstrong, N.J. Grant and K. Ishizaki (Materials Research Society, Pittsburgh, PA, 1995) **362**, p. 31.
3. E.O. Hall, *Proc. Phys. Soc. Lond.* **B64**, 747 (1951).
4. N.J. Petch, *J. Iron Steel Inst.* **174**, 25 (1953).
5. T.L. Altshuler and J.W. Christian, *Phil. Trans. Roy. Soc. Lond. A* **261**, 251 (1967).
6. R.W. Armstrong, I. Codd, R.M. Douthwaite and N.J. Petch, *Philos. Mag*., **7**, 45 (1962).
7. J.D. Embury and R.M. Fisher, *Acta Metall*. **14**, 147 (1966).
8. R.W. Armstrong, in *Yield, Flow, and Fracture of Polycrystals*, Ed. T.N. Baker (Applied. Sci. Publ., London, U.K., 1983), p. 1.
9. K. Hayashi and H. Etoh, *Mater. Trans. Japan Inst. Met*. **30**, 925 (1989).
10. J.S.C. Jang and C.C. Koch, *Scr. Met*. **24**, 1599 (1990).
11. R.W. Armstrong and S.M. Walley, *Intern. Mater. Rev.*, **53**, 105 (2008).
12. E. Orowan, *Proc. Phys. Soc. Lond*. **B52**, 8 (1940).
13. G. Schoeck, *Phys. Stat. Sol.* **8**, 499 (1965).
14. J.C.M. Li, in *Dislocation Dynamics*, Eds. A.R. Rosenfield, G.T. Hahn, A.L. Bement, Jr. and R.I. Jaffee (McGraw-Hill Book Co., N.Y., 1968) p. 87.
15. R.W. Armstrong, *(Indian) J. Sci. Indust. Res.*, **32**, 591 (1973).
16. H. Conrad, *Acta Metall.* **6**, 339 (1958).
17. H. Conrad and S. Frederick, *Acta Metall.* **10**, 1013 (1962).
18. H. Conrad, R.W. Armstrong, H. Wiedersich and G. Schoeck, *Philos. Mag.*, **6**, 177 (1961).
19. P.W. Flynn, J. Mote and J.E. Dorn, *Trans. Metall. Soc. – AIME* **221**, 1148 (1961).
20. G.A. Alers, R.W. Armstrong and J.H. Bechtold, *Trans. Metall. Soc. – AIME* **212**, 523 (1958).
21. H.L. Prekel and H. Conrad, in *Dislocation Dynamic*, Eds. A.R. Rosenfield, G.T. Hahn. A.L. Bement, Jr. and R.I. Jaffee (McGraw-Hill Book Co., N.Y., 1968) p. 431.
22. R.E. Reed, H.D. Guberman and R.W. Armstrong, *Phys. Stat. Sol.* **37**, 647 (1970).
23. F.J. Zerilli and R.W. Armstrong, *J. Appl. Phys.*, **61**, 1816 (1987).
24. F.J. Zerilli, *Metall. Mater. Trans. A* **35A**, 2547 (2004).
25. G.I. Taylor, *J. Inst. Met*. **62**, 307 (1938)
26. U.F. Kocks, *Acta Metall*. **6**, 85 (1958).
27. R.W. Armstrong, *Metall. Trans*. **1**, 1169 (1970).
28. A. Seeger, in *Dislocations and Mechanical Properties of Crystals*, Eds. J.C. Fisher, W.G. Johnston, R. Thomson and T. Vreeland, Jr. (John Wiley & Sons, Inc., N.Y., 1956) p. 243.
29. R.W. Armstrong, in *Encyclopedia of Materials: Science and Technology - Updates*, Eds. K.H.J. Buschow, R.W. Cahn, M.C. Flemings, E.J. Kramer, S. Mahajan and P. Veyssiere (Elsevier Science Ltd, Oxford, U.K., 2005) published online: Elsevier ScienceDirect.

30. R.W. Armstrong, Acta Metall., **16**, 347 (1968).
31. F.E. Hauser, P.R. Landon and J.E. Dorn, *Trans. Metal. Soc. – AIME* **206**, 589 (1956).
32. F.E. Hauser, P.R. Landon and J.E. Dorn, *Trans. Amer. Soc. Met*. **48**, 986 (1956).
33. Y.V.R.K. Prasad, N.M. Madhava and R.W. Armstrong, in *Grain Boundaries in Engineering Materials; Fourth Bolton Landing Conf.* (Claitor's Press, Baton Rouge, LA, 1974) p. 529.
34. B. Wielke, *Acta Metall*. **21**, 289 (1973).
35. Ya.M. Soifer and V.G. Shteinberg, *Phys. Stat. Sol*. **10**, K113 (1972).
36. G.W. Greenwood and A.G. Quarrell, *J. Inst. Met*. **82**, 551 (1954).
37. S.L. Mannan and P. Rodriguez, *Acta Metall*. **23**, 221 (1975)
38. R.W. Armstrong, in *Physics of Materials; A Festschrift for Dr. Walter Boas on the Occasion of His 75th Birthday*, Eds. D.W. Borland, L.M. Clarebrough and A.J.W. Moore (CSIRO and Univ. Melbourne, Australia, 1979) p. 1.
39. J.W. Wyrzykowski and M.W. Grabski, *Philos. Mag*. **53**, 505 (1986)
40. J.F. Bell, *Philos. Mag*. **11**, 1135 (1965).
41. R.P. Carreker, Jr. and W.R. Hibbard, Jr., *Acta Metall*. **1**, 654 (1953).
42. G.D. Hughes, S.D. Smith, C.S. Pande, H.R. Johnson and R.W. Armstrong, *Scr. Metall*. **20**, 93 (1986).
43. T.E. Mitchell and P.R. Thornton, *Philos. Mag*. **8**, 1127 (1963).
44. P. Feltham and J.D. Meakin *Philos. Mag*. **2**, 105 (1957).
45. M.A. Meyers, U.R. Andrade and A.H. Chokshi, *Metall. Mater. Trans. A* **26A**, 2881 (1995).
46. R.W. Armstrong and F.J. Zerilli, in *Advances in Twinning*, Eds. S. Ankem and C.S. Pande (Metall. Mater. Soc. – AIME, Warrendale, PA, 1999) p. 67.
47. R.W. Armstrong, *Eng. Fract. Mech.* **28**, 529 (1987).
48. R.M. Fisher and A.H. Cottrell, in *Relation between Structure and Mechanical Properties* (National Phys. Lab., London, U.K., 1963) p. 445.
49. N.J. Petch, in *Advances in Physical Metallurgy; Sir Alan Cottrell's 70th Birthday Meeting*, Eds. J.A. Charles and G.C. Smith (Inst. Met., London, U.K., 1990) p. 11.
50. Y.V.R.K. Prasad and R.W. Armstrong, *Philos. Mag*. **29**, 1421 (1974).
51. N.R. Risebrough and E. Teghtsoonian, *Canadian J. Phys*. **45**, 591 (1967).
52. P. Rodriguez, R.W. Armstrong, and S.L. Mannan, *Trans. Indian Inst. Met*. **56**, 189 (2003).
53. M.F. Ashby, *Philos. Mag*. **21**, 399 (1970).
54. U.F. Kocks and H. Mecking, *Prog. Mater. Sci*. **48**, 171 (2003).
55. T. Narutani and J. Takamura, *Acta Metall. Mater*. **39**, 2037 (1991).
56. P. Rodriguez, *Metall. Mater. Trans. A* **35A**, 2697 (2004).
57. W. Puschl, *Prog. Mater. Sci*. **47**, 415 (2002).
58. R.W. Armstrong, H. Conrad and F.R.N. Nabarro, in *Mechanical Properties of Nanostructured Materials and Nanocomposites*, Eds. I. Ovid'ko, C.S. Pande, R.

Krishnamoorti, E. Lavernia and G. Skandan (Mater. Res. Soc., Warrendale, PA, 2004) **791**, p. 69.
59. R.W. Armstrong and P. Rodriguez, *unpublished research* (2008).
60. J.A. del Valle and O.A. Ruano, *Scr. Mater*. **55**, 775 (2006).
61. Q. Yang and A.K. Ghosh, *Acta Mater*. **54**, 5159 (2006).
62. J.A. del Valle, F. Carreno and O. Ruano, *Acta Mater*. **54**, 4247 (2006).
63. C.H. Caceres and A.H. Blake, *Mater. Sci. Eng. A* **462**, 193 (2007).
64. R.J. Asaro and S. Suresh, *Acta Mater*. **53**, 3369 (2005).
65. R.W. Armstrong and P. Rodriguez, *Philos. Mag*., **86**, 5787 (2006).
66. A.S. Khan, B. Farrokh and L. Takacs, *J. Mater. Sci*. **43**, 3305 (2008).
67. A. Mishra, M. Martin, N.N. Thadhani, B.K. Kad, E.A. Kenik and M.A. Meyers, *Acta Mater*. **56**, 2770 (2008).
68. M.A. Meyers, A. Mishra and D.J. Benson, *Prog. Mater. Sci*. **51**, 427 (2006).
69. R.W. Armstrong, in *Dislocation Dynamics*, Eds. A.R. Rosenfield, G.T. Hahn, A.L. Bement, Jr. and R.I. Jaffee (McGraw-Hill Book Co., N.Y., 1968) p. 293.
70. R.W. Armstrong, *Canadian Metall. Quart*. **13**, 187 (1974).
71. H. Conrad, *Metall. Mater.Trans*. A **35A**, 2681 (2004).
72. N. Hansen and B. Ralph, *Acta Metall*. **30**, 411 (1982).
73. R.W. Armstrong and T.R. Smith, in *Processing and Properties of Nanocrystalline Materials*, Eds. C. Suryanarayana, J. Singh and F.H. Froes (The Metall. Soc. – AIME, Warrendale, PA, 1996) p. 345.
74. J.C.M. Li and G.C.T. Liu, *Philos. Mag*. **15**, 1059 (1967)
75. J.C.M. Li and Y.T. Chou, *Metall. Trans*. **1**, 1145 (1970).
76. R.W. Armstrong, Y.T. Chou, R.M. Fisher and N. Louat, *Philos. Mag*. **14**, 943 (1966).
77. R.W. Armstrong, *Mater. Sci. Eng. A* **409**, 24 (2005).
78. F.R.N. Nabarro, *Soviet Phys. – Sol. State Phys*. **42**, 1417 (2000).
79. J. Weertman, in *Mechanics and Materials: Fundamentals and Linkages*, Eds. M.A. Meyers, R.W. Armstrong and H.O.K. Kirchner (John Wiley & Sons, Inc., N.Y. 1999) Chap. 13, p. 451.
80. H. Conrad and J. Narayan, *Acta Mater*. **50**, 5067 (2002).
81. P. Rodriguez and R.W. Armstrong, *(Indian) Bull. Mater. Sci*. **29**, 717 (2006).
82. Q. Xia, C. Hamilton, K. Rechangel, C. Crowe and G. Collins, *Mater. Sci. Eng. Forum* **170**, 147 (1994).
83. X. Zhang, H. Wang, R.O. Scattergood, C. Koch and J. Narayan, private communication in Ref. 80.
84. C.C. Koch and J. Narayan, in *Structure and Mechanical Properties of Nanophase Materials - Theory and Computer Simulation Versus Experiment*, Eds. D. Farkas et al. (Mater. Res. Soc. Warrendale, PA, 2001) **634**, B5.1.1.
85. C.C. Koch, R.O. Scattergood, K. Linga Murty, R.K. Gudura, G. Trichy and K.V. Rajulapati, in *Mechanical Properties of Nanostructured Materials and*

Nanocomposites, Eds. I. Ovid'ko *et a*l. (Mater. Res. Soc., Warrendale, PA, 2004) **791**, p. 51.
86. K. Ogawa and K. Tanaka, *Proc. 23rd Japan Congress on Materials Research* (Soc. Mater. Sci., Japan, 1980) p. 39.
87. T.G. Langdon, *J. Mater. Sci*. **41**, 597 (2006).
88. A.A. Federov, M.Yu. Gutkin and I.A. Ovid'ko, *Acta Mater*. **51**, 887 (2003).
89. H. Conrad, *Nanotechnology* **18**, 325701 (2007).
90. F. Della Torre, P. Spatig, R. Schaublin and M. Victoria, *Acta Mater*. **5**3, 2337 (2005)
91. A.K. Ghosh, *Mater. Sci. Eng A*, DOI: 10.1016/j.msea.2006.08.122 (2006).
92. Q. Wei, *J. Mater. Sci*. **42**, 1709 (2007).
93. J.C.M. Li, *Appl. Phys. Lett*. **90**, 041912 (2007).
94. J. Narayan and Y.T. Zhu, Appl. Phys. Lett. **92**, 151908 (2008).
95. X.L. Wu, J. Narayan and Y.T. Zhu, Appl. Phys. Lett. **93**, 031910 (2008).
96. J.R. Weertman, D. Farkas, K. Hemker, H. Kung, M..Mayo, R. Mitra and H. Van Swygenhoven, *MRS Bull*. **24**, [2], 44 (1999).
97. K. Kadau, T.C. Germann, P.S. Lomdahl, B.L. Holian, D. Kadau, P. Entel, M. Kreth, F. Westerhoff and D.E. Wolf, *Metall. Mater. Trans. A* **35A**, 2719 (2004).
98. T. Zhu, J. Li, A. Samanta, H.G. Kim and S. Suresh, *Proc. Nat. Acad. Sci*. **104**, 3031 (2007).
99. R.W. Armstrong, in *Seventh Intern. Conf. on Strength of Metals and Alloys, ICSMA-CIRMA*, Eds. H.J. McQueen, J.-P. Bailon, J.I. Dickson, J.J. Jonas and M.G. Akben (Pergamon Press, Oxford, U.K., 1985) p. 195.
100. R.W. Armstrong, *Trans. Indian Inst. Met*. **50**, 521 (1997).
101. Y. Zhu, Y. Estrin, T.G. Langdon, X. Liao, T.C. Lowe, Z. Shan and R.Z. Valiev, *J. Mater. Sci.* DOI: 10.1007/s10853-008-2991-5 (2008).
102. R. Song. D. Ponge, D. Raabe, J.G. Speer and D.K. Matlock, *Mater. Sci. Eng. A* **441**, 1 (2006).
103. B. Hwang, S. Lee, Y.C. Kim, N.J. Kim and D.H. Shin, *Mater. Sci. Eng. A* **441** 308 (2006).
104. M.P. Bondar, *Comb., Explos. and Shock Waves* **44**, 365 (2008).
105. R.W. Armstrong, *Mech. Adv. Mater*., to be published (2009).